 CMES, vol.77, no.1, pp.57-80, 2011

A Spring-Damping Regularization and a Novel Lie-Group Integration Method for Nonlinear Inverse Cauchy Problems

Chein-Shan Liu[1] **and Chung-Lun Kuo**[2]

Abstract: In this paper, the solutions of inverse Cauchy problems for quasi-linear elliptic equations are resorted to an unusual mixed group-preserving scheme (MGPS). The bottom of a finite rectangle is imposed by overspecified boundary data, and we seek unknown data on the top side. The spring-damping regularization method (SDRM) is introduced by converting the governing equation into a new one, which includes a spring term and a damping term. The SDRM can further stabilize the inverse Cauchy problems, such that we can apply a direct numerical integration method to solve them by using the MGPS. Several numerical examples are examined to show that the SDRM+MGPS can overcome the ill-posed behavior of the inverse Cauchy problem. The present algorithm has good efficiency and stability against the disturbance from random noise, even with an intensity being large up to 10%, and the computational time is very saving.

Keywords: Inverse Cauchy problem, Quasi-linear elliptic equations, Spring-damping regularization method, Mixed group-preserving scheme

1 Introduction

During the past several decades, the science and engineering communities have paid much attention to the inverse Cauchy problem, which is a non-characteristic initial value problem for the elliptic type partial differential equation (PDE). According to the Cauchy-Kowalewski theorem, the solution of an analytic Cauchy problem for PDEs exists and is unique. However, the Cauchy problem is quite difficult to solve both numerically and analytically, since its solution does not depend continuously on the given data, that is, a small error in the specified data may result in a terribly incorrect solution. It means that the continuous dependence of the so-

[1] Department of Civil Engineering, National Taiwan University, Taipei, Taiwan
[2] Department of Systems Engineering and Naval Architecture, National Taiwan Ocean University, Keelung, Taiwan. Corresponding author: E-mail: D96510001@mail.ntou.edu.tw

lution on the given data is not satisfied in the Hardmard sense. Therefore, we must treat this type problem with a suitable numerical algorithm, which compromises accuracy and stability.

The use of electrostatic image in the non-destructive testing of metallic structures leads to an inverse boundary value problem for elliptic equation. In order to detect the unknown shape of the inclusion within a conducting metal, the overspecified Cauchy data, for example the voltage and current, are imposed on the accessible boundary [Akduman and Kress (2002); Inglese (1997); Kaup, Santosa and Vogelius (1996)]. This amounts to solving an inverse Cauchy problem from available data measured on the partial boundary. There had been many studies on this type problems in the open literature [Andrieux, Maranger and Ben Abda (2006); Aparicio and Pidcock (1996); Ben Belgacem and El Fekih (2005); Berntsson and Eldén (2001); Bourgeois (2005, 2006); Chapko and Kress (2005); Kress (2004); Mera, Elliott, Ingham and Lesnic (2000); Slodička and Van Keer (2004); Liu (2011)].

In the past several years there already had many numerical methods being proposed to solve the inverse Cauchy problems [Brühl and Hanke (2000); Cimetière, Delvare, Jaoua and Pons (2001); Fang and Lu (2004); Knowles (1998); Chang, Yeih and Shieh (2001); Chi, Yeih and Liu (2009); Johansson and Marin (2010)]. Among the many numerical methods, the schemes based on iteration have also been developed previously by Jourhmane and Nachaoui (1999, 2002), Essaouini, Nachaoui and Hajji (2004), Nachaoui (2004), Jourhmane, Lesnic, and Mera (2004), and Marin (2009).

Liu (2008a) has applied a modified collocation Trefftz method in the inverse Cauchy problem for the Laplace equation. In order to achieve a stable numerical solution for recovering the discontinuous data, a regularization by truncating the higher modes of the Fourier series of the input data is necessary. A similar method has been named the Fourier regularization method by Fu, Li, Qian and Xiong (2008).

Most of the existent literature were concerned with the inverse Cauchy problems of linear elliptic equations, like as, the Laplace equation [Ling and Takeuchi (2008); Liu (2008a, 2008b); Marin (2009); Shigeta and Young (2009); Qian, Fu and Xiong (2006); Xiong and Fu (2006); Qian and Wu (2009); Tuan, Trong and Quan (2010); Abbasbandy and Hashemi (2011), Liu (2011)], the Poisson equation [Marin (2008)], the Helmholtz equation [Qin and Wei (2009); Qin, Wei and Shi (2009); Johansson and Marin (2010); Cheng, Fu and Feng (2011); Zhang, Qin and Wei (2011)], and the biharmonic equation [Liu (2008c)]. To account of the sensitivity to noisy disturbance of the inverse Cauchy problems for linearly elliptic PDEs, there already had many studies by using different regularization techniques, such as the Tikhonov regularization, linear regularization and their variants [Wei, Hon and Ling (2007); Chen, Chen and Lee (2009)]. Regularization techniques were created one by one, but they are only useful for each specific case being considered. There are two major drawbacks of the previous approaches: some kind of matrix inversion is required for the resulting ill-conditioned matrix, and they cannot be directly extended to nonlinear elliptic systems.

In contrast to those methods the present paper aims to provide a simple numerical computation method based on an unusual group-preserving scheme, directly integrating the inverse Cauchy problem as an initial value problem. In order to express the new method simpler and clearer we first restrict ourself to the inverse Cauchy problem defined in a rectangle, because in this domain a numerical method of lines is easily employed for the discretization of the nonlinear elliptic equation into a nonlinear system of ODEs. It is known that the inverse Cauchy problem is a non-characteristic problem, and there were rare papers to develop a direct numerical integration method to solve it [Qian, Fu and Xiong (2006); Abbasbandy and Hashemi (2011); Liu and Chang (2012)]. After a suitable and mathematically equivalent regularization technique for the enhancement of numerical stability by introducing the spring/damping terms in Section 2, we develop a numerical integration method for the inverse Cauchy problem of nonlinear elliptic equation defined in a rectangular domain, which is discretized into a nonlinear ODEs system by using the numerical method of lines in Section 3. In Section 4 we introduce three different group-preserving schemes, and the numerical results are given in Section 5. Finally, the conclusions are given in Section 6.

2 A spring-damping regularization

We consider an inverse Cauchy problem for a quasi-linear elliptic equation with overspecified boundary conditions at $y=0$:

$$\frac{\partial^2 u}{\partial x^2}+\frac{\partial^2 u}{\partial y^2}=F(x,y,u,u_x,u_y),\ \ 0<x<\ell,\ \ 0<y<b, \tag{1}$$

$$u(x,0)=f(x),\ \ 0\leq x\leq \ell, \tag{2}$$

$$\frac{\partial u}{\partial y}(x,0)=g(x),\ \ 0\leq x\leq \ell, \tag{3}$$

$$u(0,y)=u_0(y),\ \ u(\ell,y)=u_\ell(y),\ \ 0\leq y\leq b, \tag{4}$$

where $f(x), g(x), u_0(y)$, and $u_\ell(y)$ are given functions.

In the present paper we develop a novel integration method to directly solve the above inverse Cauchy problem by recovering the data at the top side $y=b$. The integration direction will be in the y-axis, and thus we consider the following variable transformation:

$$u(x,y) = e^{\alpha y} U(x,y). \tag{5}$$

A similar transformation has been used by Liu (2004) to treat the backward heat conduction problem. From Eqs. (1)-(5) it follows that

$$\frac{\partial^2 U}{\partial x^2} + \frac{\partial^2 U}{\partial y^2} + 2\alpha \frac{\partial U}{\partial y} + \alpha^2 U = e^{-\alpha y} F(x, y, e^{\alpha y} U, e^{\alpha y} U_x, e^{\alpha y} U_y + \alpha e^{\alpha y} U), \tag{6}$$

$$U(x,0) = f(x), \ \ 0 \le x \le \ell, \tag{7}$$

$$\frac{\partial U}{\partial y}(x,0) = g(x) - \alpha f(x), \ \ 0 \le x \le \ell, \tag{8}$$

$$U(0,y) = U_0(y) = e^{-\alpha y} u_0(y), \ \ U(\ell,y) = U_\ell(y) = e^{-\alpha y} u_\ell(y), \ \ 0 \le y \le b. \tag{9}$$

It can be seen that in Eq. (6) we have introduced two extra terms: a spring term $\alpha^2 U$, and a damping term $2\alpha \partial U / \partial y$. It is known that in the mechanical vibration system a suitable choice of spring and damping constants can enhance the stability of motion. This regularization technique has been first developed by Liu and Chang (2012) for linear inverse Cauchy problems defined in annular domains, which was shown to be very effective for overcoming the ill-posed behavior of inverse Cauchy problems. In the present paper we are going to extend the spring-damping regularization method (SDRM) to the nonlinear inverse Cauchy problems.

3 Numerical method of lines

The numerical method of lines is simple in concept that for a given system of partial differential equations discretize all but one of the independent variables. The semi-discrete procedure yields a coupled system of ordinary differential equations which are then numerically integrated. For the above equation (6) we adopt the numerical method of lines to discretize the spatial coordinate x by

$$\left.\frac{\partial U(x,y)}{\partial x}\right|_{x=i\Delta x} = \frac{U_{i+1}(y) - U_{i-1}(y)}{2\Delta x},$$

$$\left.\frac{\partial^2 U(x,y)}{\partial x^2}\right|_{x=i\Delta x} = \frac{U_{i+1}(y) - 2U_i(y) + U_{i-1}(y)}{(\Delta x)^2},$$

where $\Delta x = \ell/(n+1)$ is a uniform discretization spacing length, and $U_i(y) = U(i\Delta x, y)$, such that Eq. (6) can be approximated by

$$\frac{\partial U_i(y)}{\partial y} = V_i(y), \tag{10}$$

$$\frac{\partial V_i(y)}{\partial y} = -\frac{U_{i+1}(y) - 2U_i(y) + U_{i-1}(y)}{(\Delta x)^2} - 2\alpha V_i(y) - \alpha^2 U_i(y) + e^{-\alpha y} F_i(y), \tag{11}$$

where for simple notation we use $F_i(y)$ to denote

$$F(x_i, y, e^{\alpha y} U_i(y), (U_{i+1}(y) - U_{i-1}(y))/(2\Delta x),\ e^{\alpha y} V_i(y) + \alpha e^{\alpha y} U_i(y)).$$

The next step is to advance the solution from the initial conditions given at $y = 0$ to the position $y = b$. Really, Eqs. (10) and (11) have totally $2n$ coupled nonlinear differential equations for the $2n$ variables $U_i(y), V_i(y), i = 1, 2, \ldots, n$, which can be numerically integrated to obtain the solutions.

4 Group-preserving schemes

Liu (2001) has derived a Lie-group transformation for the augmented dynamics on the future cone, and developed a group-preserving scheme for an effective numerical solution of nonlinear differential equations.

4.1 Forward group-preserving scheme

Group-preserving scheme (GPS) can preserve the internal symmetry group of the considered nonlinear differential equations system. Liu (2001) has embedded it into an augmented dynamical system, which concerns with not only the evolution of state variables but also the evolution of the magnitude of state variables vector. That is, for an n ODEs system:

$$\dot{\mathbf{x}} = \mathbf{f}(\mathbf{x}, t), \;\; \mathbf{x} \in \mathbb{R}^n, \;\; t \in \mathbb{R}, \tag{12}$$

we can embed it to the following $n+1$-dimensional augmented dynamical system:

$$\frac{d}{dt} \begin{bmatrix} \mathbf{x} \\ \|\mathbf{x}\| \end{bmatrix} = \begin{bmatrix} \mathbf{0}_{n\times n} & \frac{\mathbf{f}(\mathbf{x},t)}{\|\mathbf{x}\|} \\ \frac{\mathbf{f}^{\mathrm{T}}(\mathbf{x},t)}{\|\mathbf{x}\|} & 0 \end{bmatrix} \begin{bmatrix} \mathbf{x} \\ \|\mathbf{x}\| \end{bmatrix}. \tag{13}$$

Here we assume $\|\mathbf{x}\| > 0$ and hence the above system is well-defined.

It is obvious that the first row in Eq. (13) is the same as the original equation (12), but the inclusion of the second row in Eq. (13) gives us a Minkowskian structure of the augmented state variables of $\mathbf{X} := (\mathbf{x}^{\mathrm{T}}, \|\mathbf{x}\|)^{\mathrm{T}}$, satisfying a future cone condition:

$$\mathbf{X}^{\mathrm{T}}\mathbf{g}\mathbf{X} = 0, \tag{14}$$

where

$$\mathbf{g} = \begin{bmatrix} \mathbf{I}_n & \mathbf{0}_{n\times 1} \\ \mathbf{0}_{1\times n} & -1 \end{bmatrix} \tag{15}$$

is a Minkowski metric, $\mathbf{I}_n$ is the identity matrix of order n, and the superscript T stands for the transpose. In terms of $(\mathbf{x}, \|\mathbf{x}\|)$, Eq. (14) becomes

$$\mathbf{X}^{\mathrm{T}}\mathbf{g}\mathbf{X} = \mathbf{x}\cdot\mathbf{x} - \|\mathbf{x}\|^2 = \|\mathbf{x}\|^2 - \|\mathbf{x}\|^2 = 0, \tag{16}$$

where the dot between two n-dimensional vectors denotes their Euclidean inner product. The cone condition is thus the most natural constraint that we can impose on the dynamical system (13).

Consequently, we have an $n+1$-dimensional augmented system:

$$\dot{\mathbf{X}} = \mathbf{A}\mathbf{X} \tag{17}$$

with a constraint (14), where

$$\mathbf{A} := \begin{bmatrix} \mathbf{0}_{n\times n} & \frac{\mathbf{f}(\mathbf{x},t)}{\|\mathbf{x}\|} \\ \frac{\mathbf{f}^{\mathrm{T}}(\mathbf{x},t)}{\|\mathbf{x}\|} & 0 \end{bmatrix}, \tag{18}$$

satisfying

$$\mathbf{A}^{\mathrm{T}}\mathbf{g} + \mathbf{g}\mathbf{A} = \mathbf{0}, \tag{19}$$

is a Lie algebra $so(n,1)$ of the proper orthochronous Lorentz group $SO_o(n,1)$. This fact prompts us to devise the so-called group-preserving scheme, whose discretized mapping $\mathbf{G}$ exactly preserves the following properties:

$$\mathbf{G}^{\mathrm{T}}\mathbf{g}\mathbf{G} = \mathbf{g}, \tag{20}$$

$$\det \mathbf{G} = 1, \tag{21}$$

$$G_0^0 > 0, \tag{22}$$

where G_0^0 is the 00th component of $\mathbf{G}$.

We assume that the value of $\mathbf{A}$ at the k-th time step is denoted by $\mathbf{A}(k)$, which is viewed as a constant matrix. An exponential mapping of $\mathbf{A}(k)$ admits a closed-form representation:

$$\exp[h\mathbf{A}(k)] = \begin{bmatrix} \mathbf{I}_n + \frac{(a_k-1)}{\|\mathbf{f}_k\|^2}\mathbf{f}_k\mathbf{f}_k^{\mathrm{T}} & \frac{b_k\mathbf{f}_k}{\|\mathbf{f}_k\|} \\ \frac{b_k\mathbf{f}_k^{\mathrm{T}}}{\|\mathbf{f}_k\|} & a_k \end{bmatrix}, \tag{23}$$

where

$$a_k := \cosh\left(\frac{h\|\mathbf{f}_k\|}{\|\mathbf{x}_k\|}\right), \quad b_k := \sinh\left(\frac{h\|\mathbf{f}_k\|}{\|\mathbf{x}_k\|}\right). \tag{24}$$

Consequently, we can obtain

$$\mathbf{x}_{k+1} = \mathbf{x}_k + \eta_1(k)\mathbf{f}_k = \mathbf{x}_k + \frac{(a_k-1)\mathbf{f}_k\cdot\mathbf{x}_k + b_k\|\mathbf{x}_k\|\|\mathbf{f}_k\|}{\|\mathbf{f}_k\|^2}\mathbf{f}_k. \tag{25}$$

This scheme preserves all the group properties for all $h > 0$, which is called a *forward group-preserving scheme*.

4.2 Backward group-preserving scheme

We can also embed Eq. (12) into the following $n+1$-dimensional augmented dynamical system:

$$\frac{d}{dt}\begin{bmatrix} \mathbf{x} \\ -\|\mathbf{x}\| \end{bmatrix} = \begin{bmatrix} \mathbf{0}_{n\times n} & -\frac{\mathbf{f}(\mathbf{x},t)}{\|\mathbf{x}\|} \\ -\frac{\mathbf{f}^{\mathrm{T}}(\mathbf{x},t)}{\|\mathbf{x}\|} & 0 \end{bmatrix}\begin{bmatrix} \mathbf{x} \\ -\|\mathbf{x}\| \end{bmatrix}. \tag{26}$$

It is obvious that the first equation in Eq. (26) is the same as the original equation (12), but the inclusion of the second equation gives us a Minkowskian structure of the augmented state variables of $\mathbf{X} := (\mathbf{x}^{\mathrm{T}}, -\|\mathbf{x}\|)^{\mathrm{T}}$, satisfying a past cone condition:

$$\mathbf{X}^{\mathrm{T}}\mathbf{g}\mathbf{X} = \mathbf{x}\cdot\mathbf{x} - (-\|\mathbf{x}\|)^2 = \|\mathbf{x}\|^2 - \|\mathbf{x}\|^2 = 0. \tag{27}$$

Here, we should stress that the cone condition imposed on the dynamical system (13) is a future cone, and that for the dynamical system (26) the imposed cone condition (27) is a past cone.

Consequently, we have an $n+1$-dimensional augmented system:

$$\dot{\mathbf{X}} = \mathbf{B}\mathbf{X} \tag{28}$$

with a constraint (27), where

$$\mathbf{B} := \begin{bmatrix} \mathbf{0}_{n\times n} & -\frac{\mathbf{f}(\mathbf{x},t)}{\|\mathbf{x}\|} \\ -\frac{\mathbf{f}^{\mathrm{T}}(\mathbf{x},t)}{\|\mathbf{x}\|} & 0 \end{bmatrix} \tag{29}$$

satisfying

$$\mathbf{B}^{\mathrm{T}}\mathbf{g} + \mathbf{g}\mathbf{B} = \mathbf{0}, \tag{30}$$

is a Lie algebra $so(n,1)$ of the proper orthochronous Lorentz group $SO_o(n,1)$. The term orthochronous used in the special relativity theory is referred to the preservation of time orientation. However, it should be understood here as the preservation of the sign of $-\|\mathbf{x}\|$.

Similarly, we assume that the value of $\mathbf{B}$ at the k-th time step is denoted by $\mathbf{B}(k)$, which is viewed as a constant matrix. Accordingly, an exponential mapping of $\mathbf{B}(k)$ admits a closed-form representation:

$$\exp[-h\mathbf{B}(k)] = \begin{bmatrix} \mathbf{I}_n + \frac{(a_k-1)}{\|\mathbf{f}_k\|^2}\mathbf{f}_k\mathbf{f}_k^{\mathrm{T}} & \frac{b_k\mathbf{f}_k}{\|\mathbf{f}_k\|} \\ \frac{b_k\mathbf{f}_k^{\mathrm{T}}}{\|\mathbf{f}_k\|} & a_k \end{bmatrix}, \tag{31}$$

where a_k and b_k were defined by Eq. (24), and we have

$$\mathbf{x}_{k-1} = \mathbf{x}_k + \eta_2(k)\mathbf{f}_k = \mathbf{x}_k + \frac{(a_k-1)\mathbf{f}_k\cdot\mathbf{x}_k - b_k\|\mathbf{x}_k\|\|\mathbf{f}_k\|}{\|\mathbf{f}_k\|^2}\mathbf{f}_k. \tag{32}$$

This scheme is group properties preserved for all $h > 0$. This scheme was first developed by Liu, Chang and Chang (2006), and was called a *backward group-preserving scheme*.

Comparing Eqs. (32) and (25) it is interesting to note that these two numerical schemes have the same form in addition that the sign before $b_k\|\mathbf{x}_k\|\|\mathbf{f}_k\|$ in the numerators.

4.3 Mixed group-preserving scheme

Although the above two schemes, *forward and backward group-preserving schemes*, are very accurate, but they are sensitive to the noise, which is added on the data by

$$\hat{f}_i = f(x_i)[1+\sigma R(i)], \quad \hat{g}_i = g(x_i)[1+\sigma R(i)], \tag{33}$$

where $R(i)$ are random numbers in $[-1,1]$. In order to overcome this instability we apply the following mixed group-preserving scheme (MGPS) to Eqs. (10) and (11):

$$U_i(y_{j+1}) = U_i(y_j) + \eta_1(j)V_i(y_j), \tag{34}$$

$$V_i(y_{j+1}) = V_i(y_j) + \eta_2(j)H_i(y_j), \tag{35}$$

where

$$H_i(y) := -\frac{U_{i+1}(y) - 2U_i(y) + U_{i-1}(y)}{(\Delta x)^2} - 2\alpha V_i(y) - \alpha^2 U_i(y) + e^{-\alpha y} F_i(y), \tag{36}$$

and $\eta_1(j)$ and $\eta_2(j)$ are defined respectively in Eqs. (25) and (32). Here, instead of $\eta_1(j)$ used in the forward group-preserving scheme, the term $\eta_2(j)$ used in Eq. (35) can impress the instability which is happened for the forward group-preserving scheme.

5 Numerical examples

5.1 Example 1

In this example we apply schemes (25) and (32), respectively, to

$$u_{xx} + u_{yy} = 0, \;\; 0 < x < \pi, \;\; 0 < y < 1, \tag{37}$$

$$u(x,0) = \sin x, \;\; u_y(x,0) = 0, \tag{38}$$

$$u(0,y) = u(\pi,y) = 0. \tag{39}$$

The exact solution is $u(x,y) = \sin x \cosh y$. Without considering the noise being imposed on the given initial data, we can obtain very accurate results as shown in Fig. 1, where $\Delta x = \pi/40$, and $h = \Delta y = 10^{-4}$ are used in the GPS. Because this problem is symmetric with y and $-y$, and the boundary conditions are independent to y, both schemes led to the same results. However, when a little noise is imposed on the given data, both schemes are failure to recover the data on the top side.

5.2 Example 2

In this example we apply schemes (34) and (35) to

$$u_{xx} + u_{yy} = 0, \;\; 0 < x < \pi, \;\; 0 < y < 1, \tag{40}$$

$$u(x,0) = 0, \;\; u_y(x,0) = \sin x, \tag{41}$$

$$u(0,y) = u(\pi,y) = 0. \tag{42}$$

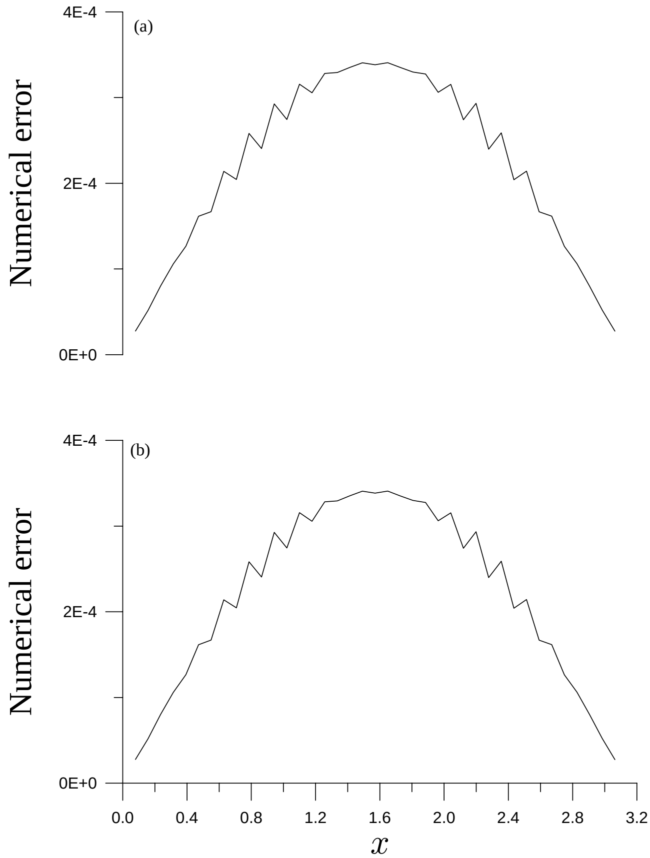

Figure 1: For example 1 displaying numerical errors by using (a) forward and (b) backward group-preserving schemes.

The exact solution is $u(x,y) = \sin x \sinh y$. Under a large noise with $\sigma = 10\%$, and with $\Delta x = \pi/100$, $\Delta y = 1/2000$ used in the MGPS, the numerical solutions at $y = 1$ are compared with the exact ones in Fig. 2, where $\alpha = 0.165$ is used. It can be seen that the present algorithm is quite robust, which can recover the data on the top side very accurately, even under a large noise.

Now, we explain the effect of α in the formulation. The original equation for the

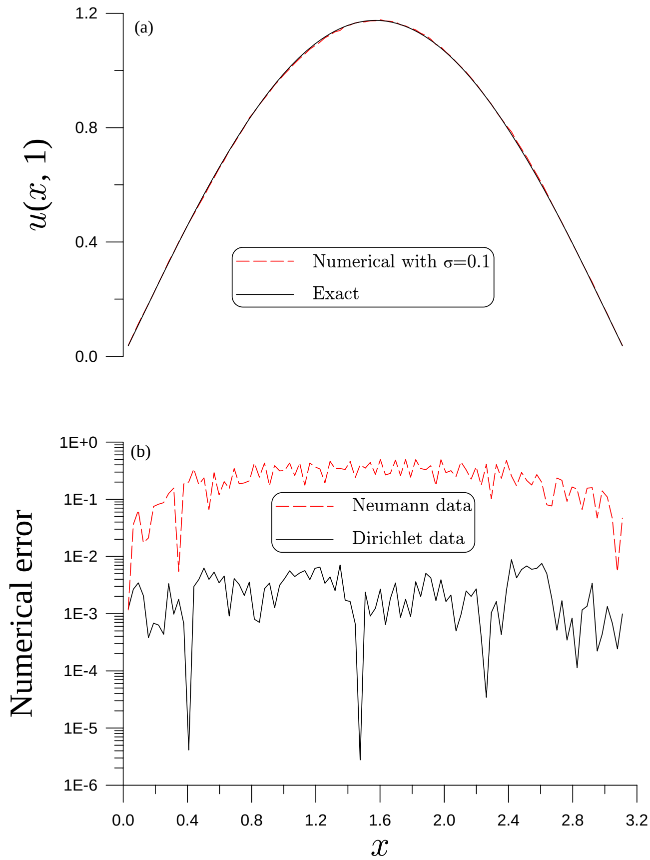

Figure 2: For example 2: (a) comparing numerical and exact solutions, and (b) displaying numerical errors of Dirichlet and Neumann data.

Laplace equation as discretized for x is

$$\frac{d}{dy}\begin{bmatrix}\mathbf{u}\\ \mathbf{v}\end{bmatrix}=\begin{bmatrix}\mathbf{0}_{n\times n} & \mathbf{I}_n\\ \mathbf{C}_{n\times n} & \mathbf{0}_{n\times n}\end{bmatrix}\begin{bmatrix}\mathbf{u}\\ \mathbf{v}\end{bmatrix}+\begin{bmatrix}\mathbf{0}_{n\times 1}\\ -\frac{u_0}{(\Delta x)^2}\\ 0\\ \vdots\\ 0\\ -\frac{u_{n+1}}{(\Delta x)^2}\end{bmatrix}=\mathbf{A}_1\begin{bmatrix}\mathbf{u}\\ \mathbf{v}\end{bmatrix}+\mathbf{F}_1, \tag{43}$$

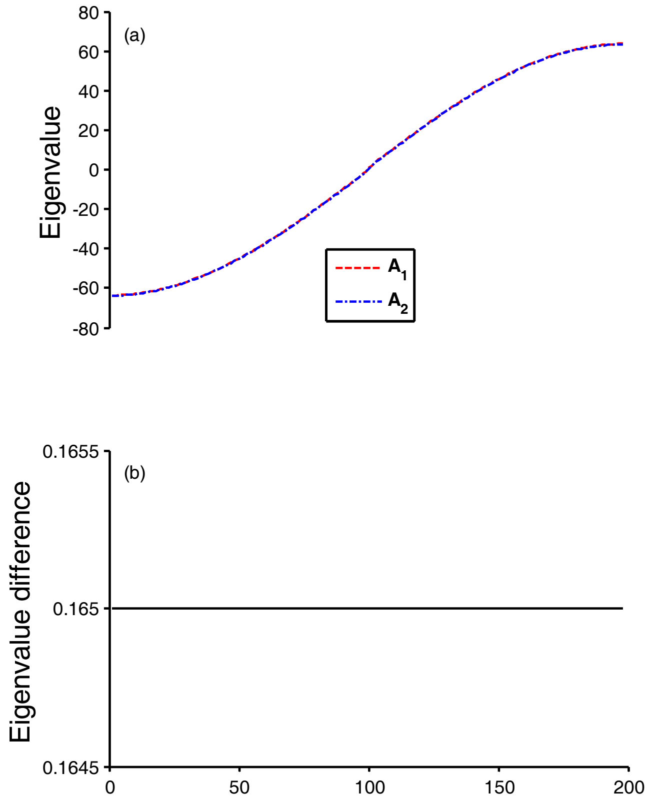

Figure 3: For example 2: (a) comparing the eigenvalues of the original and the transformed system, and (b) showing the difference of the eigenvalues.

where **C** is the central difference matrix:

$$\mathbf{C} = \frac{1}{(\Delta x)^2} \begin{bmatrix} 2 & -1 & & & & \\ -1 & 2 & -1 & & & \\ & \cdot & \cdot & \cdot & & \\ & & \cdot & \cdot & \cdot & \\ & & & \cdot & \cdot & \cdot \\ & & & & -1 & 2 \end{bmatrix}, \tag{44}$$

and $\mathbf{u} = (u_1, \dots, u_n)^{\mathrm{T}}$ and $\mathbf{v} = (v_1, \dots, v_n)^{\mathrm{T}}$. However, for the transformed equation

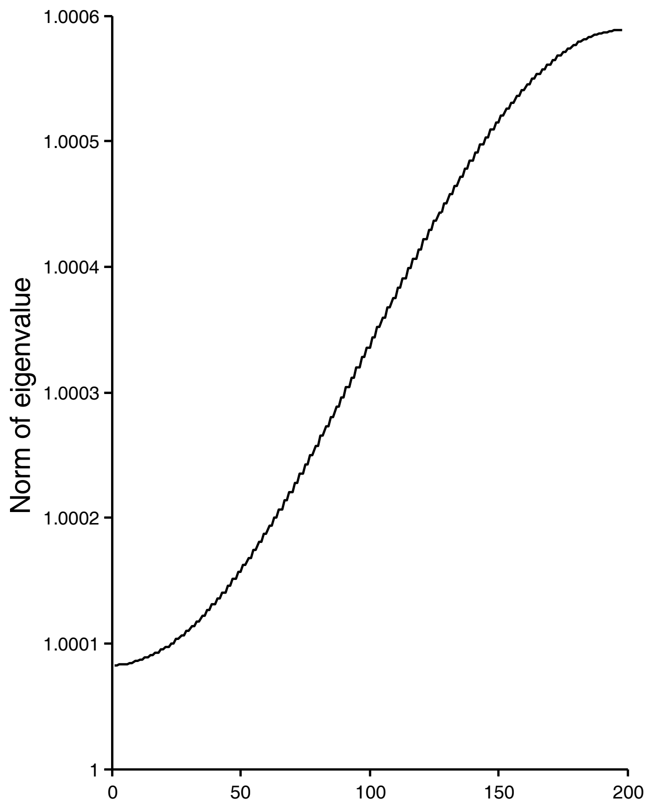

Figure 4: For example 2 displaying the moduli of the eigenvalues of the mapping matrix at the first step.

we have

$$\frac{d}{dy}\begin{bmatrix} \mathbf{U} \\ \mathbf{V} \end{bmatrix} = \begin{bmatrix} \mathbf{0}_{n\times n} & \mathbf{I}_n \\ \mathbf{C}_{n\times n}-\alpha^2\mathbf{I}_n & -2\alpha\mathbf{I}_n \end{bmatrix}\begin{bmatrix} \mathbf{U} \\ \mathbf{V} \end{bmatrix} + \begin{bmatrix} \mathbf{0}_{n\times 1} \\ -\frac{U_0}{(\Delta x)^2} \\ 0 \\ \vdots \\ 0 \\ -\frac{U_{n+1}}{(\Delta x)^2} \end{bmatrix} = \mathbf{A}_2\begin{bmatrix} \mathbf{U} \\ \mathbf{V} \end{bmatrix} + \mathbf{F}_2, \tag{45}$$

where $\mathbf{U} = (U_1,\ldots,U_n)^{\mathrm{T}}$ and $\mathbf{V} = (V_1,\ldots,V_n)^{\mathrm{T}}$. For this case we compare the eigenvalues of $\mathbf{A}_1$ and $\mathbf{A}_2$ in Fig. 3(a), of which the eigenvalues of $\mathbf{A}_2$ are smaller than those of $\mathbf{A}_1$ as shown in Fig. 3(b) with a quantity $\alpha = 0.165$.

More importantly, we can check the stability of the new MGPS algorithm in Eqs. (34) and (35) for this example. Through some derivations we can obtain

$$\begin{bmatrix} \mathbf{U}^{j+1} \\ \mathbf{V}^{j+1} \end{bmatrix} = \begin{bmatrix} \mathbf{I}_n & \eta_1(j)\mathbf{I}_n \\ \eta_2(j)(\mathbf{C}_{n\times n} - \alpha^2\mathbf{I}_n) & [1-2\alpha\eta_2(j)]\mathbf{I}_n \end{bmatrix} \begin{bmatrix} \mathbf{U}^{j} \\ \mathbf{V}^{j} \end{bmatrix} + \begin{bmatrix} \mathbf{0}_{n\times 1} \\ -\frac{\eta_2(j)U_0^j}{(\Delta x)^2} \\ 0 \\ \vdots \\ 0 \\ -\frac{\eta_2(j)U_{n+1}^j}{(\Delta x)^2} \end{bmatrix}$$

$$= \mathbf{A}_3^j \begin{bmatrix} \mathbf{U}^{j} \\ \mathbf{V}^{j} \end{bmatrix} + \mathbf{F}_3^j. \tag{46}$$

As we know, the method is stable if the above mapping matrix $\mathbf{A}_3^j$ with its eigenvalues having the moduli smaller than or equal to unity. By applying a mathematical code in the MatLab we can compute the eigenvalues of $\mathbf{A}_3^j$ for each integration step. However, as a representative case, we only compute the eigenvalues of $\mathbf{A}_3^1$ at the first step. In Fig. 4, we plot the moduli of the eigenvalues. It can be seen that all the moduli of the eigenvalues are only slightly greater than 1. This is the main reason that the present algorithm allows us using a direct integration method to solve the inverse Cauchy problem.

5.3 Example 3

In this example we apply schemes (34) and (35) to

$$u_{xx} + u_{yy} = 0, \quad -1 < x < 1, \;\; 0 < y < 1,$$
$$u(x,y) = \exp(y^2 - x^2)\cos(2xy). \tag{47}$$

Under a large noise with $\sigma = 10\%$, and with $\Delta x = 2/60$, $\Delta y = 1/1000$ used in the MGPS, the numerical solution at $y = 1$ is compared with the exact one in Fig. 5, where $\alpha = 0.925$ is used. It can be seen that the present algorithm is quite robust, which can recover the data at the top side very well, even under a large noise.

5.4 Example 4

The following nonlinear Helmholtz equation is investigated:

$$u_{xx} + u_{yy} = 4u^3. \tag{48}$$

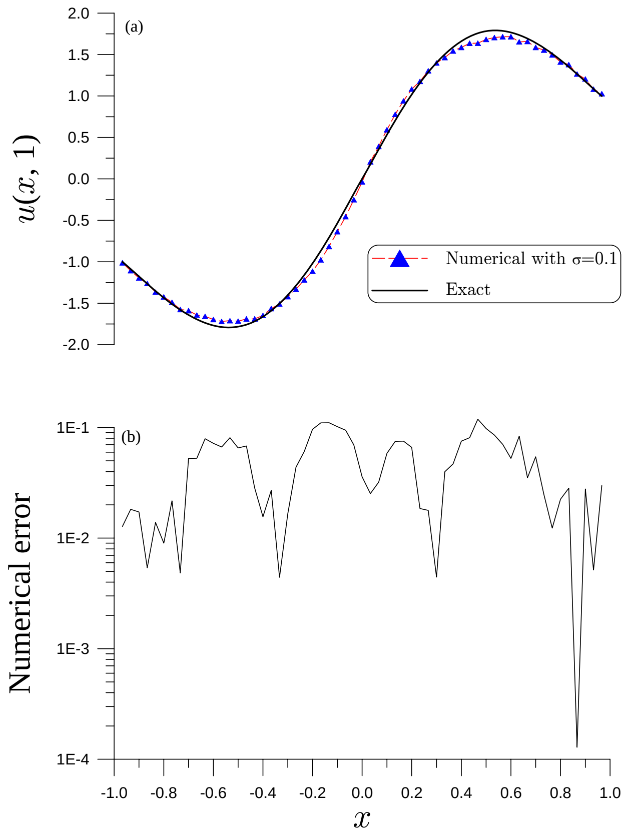

Figure 5: For example 3: (a) comparing numerical and exact solutions, and (b) displaying numerical error of Dirichlet data.

The domain is same as that given in Example 2. The analytic solution

$$u(x,y) = \frac{1}{x+y+4} \tag{49}$$

is singular on the straight line $x+y=-4$. Under the noises with $\sigma = 1\%$ and $\sigma = 2\%$, and with $\Delta x = 1/30$, $\Delta y = 1/3000$ used in the MGPS, the numerical errors for the solutions at $y=1$ are shown in Fig. 6, where $\alpha = -0.25$ is used. It can be seen that the present algorithm is quite robust, which can recover the data rather well.

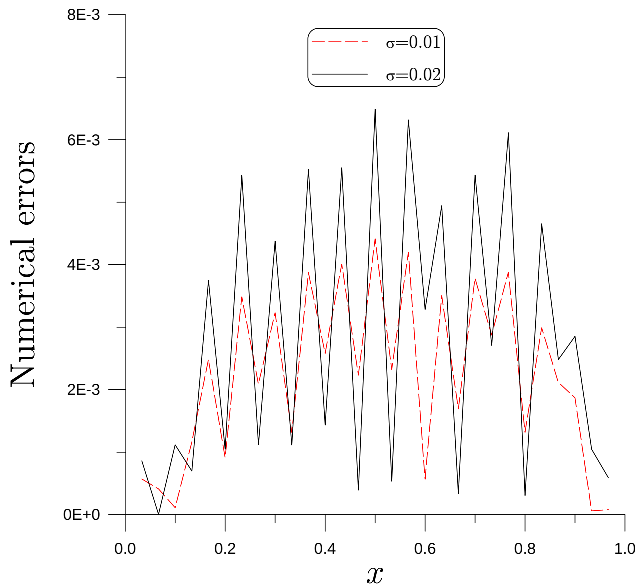

Figure 6: For example 4 displaying numerical errors of Dirichlet data.

5.5 *Example 5*

In this example we apply schemes (34) and (35) to the following quasi-linear PDE:

$$\nabla \cdot (e^u \nabla u) = 0, \quad 0 < x < 1, \quad 0 < y < 1, \tag{50}$$

$$u = \ln(2 + x^2 - y^2). \tag{51}$$

Essaouini, Nachaoui and Hajji (2004) have computed this problem by an iterative boundary element procedure. The required data can be computed from Eq. (51). Under a noise with $\sigma = 10\%$, and with $\Delta x = 1/40$, $\Delta y = 1/5000$ used in the MGPS, the numerical solution at $y = 1$ is compared with the exact one in Fig. 7, where $\alpha = 0.98$ is used. It can be seen that the present algorithm can recover the data with a reasonable accuracy even under a large noise for the nonlinear problem.

5.6 *Example 6*

In this example we apply schemes (34) and (35) to a more ill-posed case of

$$u_{xx} + u_{yy} = y^2, \quad 0 < x < 0.05, \quad 0 < y < 0.45, \tag{52}$$

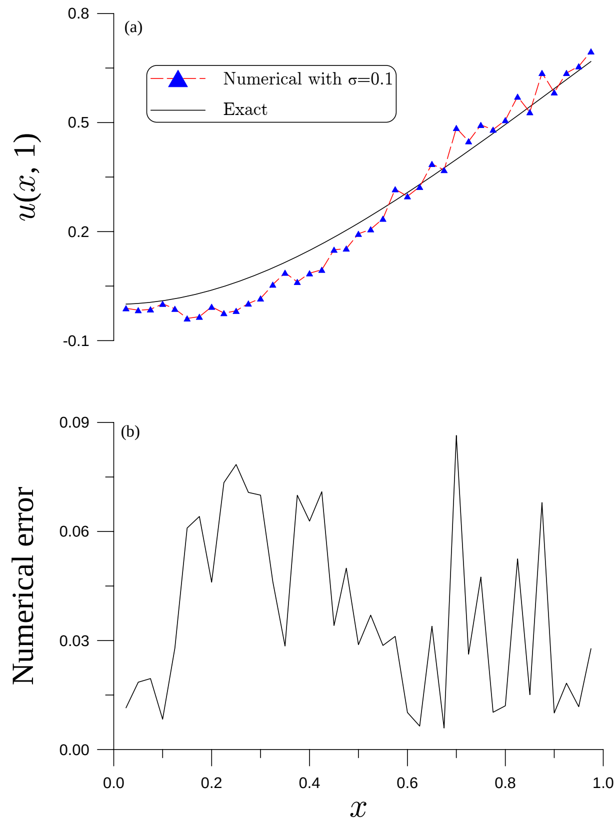

Figure 7: For example 5: (a) comparing numerical and exact solutions, and (b) displaying numerical error of Dirichlet data.

where the exact solution is

$$u(x,y) = \exp(y)(y\cos x - x\sin x) + \frac{y^4}{12}. \tag{53}$$

Under the following conditions:

$$u(x,0) = -x\sin x, \quad u_y(x,0) = -x\sin x + \cos x, \quad 0 < x < 0.05, \tag{54}$$

$$u(0,y) = y\exp(y) + \frac{y^4}{12}, \quad 0 < y < 0.45, \tag{55}$$

we attempt to recover the Dirichlet data $u(x = 0.05, y)$ and $u(x, y = 0.45)$. It can be seen that the overspecified data are only given on a small part with only five

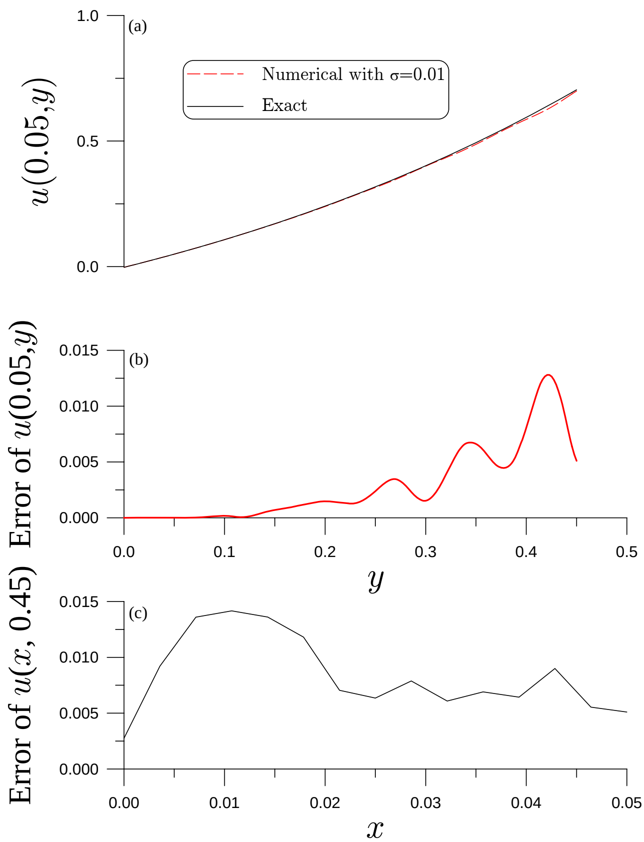

Figure 8: For example 6: (a) comparing numerical and exact solutions, and (b) and (c) displaying numerical errors of Dirichlet data.

percentages of the total boundary, and it is given no data on one-half of the total boundary.

Under a noise with $\sigma = 1\%$, and with $\Delta x = 0.05/14$, $\Delta y = 0.45/200$ and $\alpha = 1$ used in the MGPS, the numerical solution at $x = 0.05$ is compared with the exact one in Fig. 8(a), where the maximum error is about 0.02 as shown in Fig. 8(b). In Fig. 8(c) we show the numerical error of $u(x, y = 0.45)$ where the maximum error is about 0.016. It can be seen that the present algorithm can recover one-half data very accurately.

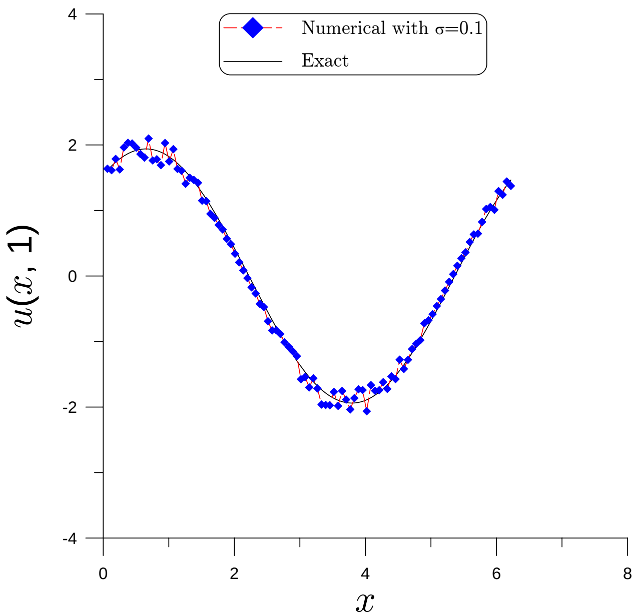

Figure 9: For example 7 comparing numerical and exact solutions

5.7 *Example 7*

In this example we consider

$$u_{xx} + u_{yy} = 0, \quad 0 < x < 2\pi, \quad 0 < y < 1,$$
$$u(x,y) = \sin x \sinh y + \cos x \cosh y. \tag{56}$$

We attempt to recover the Dirichlet data $u(x, y = 1)$. Under a large noise with $\sigma = 10\%$, and with $\Delta x = 2\pi/60$, $\Delta y = 1/1000$ and $\alpha = 1$ used in the MGPS, the numerical solution at $y = 1$ is compared with the exact one in Fig. 9. In order to further stabilize this computation we have inserted a factor $\beta = 0.3$ before η_1 and η_2 in Eqs. (34) and (35).

6 Conclusions

By employing a variable transformation and the mixed group-preserving scheme (MGPS) we can recover the missing data on the top side very well for a nonlinear inverse Cauchy problem. The variable α plays both a spring and a damping constant, which can stabilize the numerical solutions. Several numerical examples of the inverse Cauchy problem were worked out, which show that our numerical integration methods are applicable to the inverse Cauchy problem, even for the very severely ill-posed ones. Under the overspecified data with a quite large noise the MGPS together with the spring-damping regularization method (SDRM) was also robust enough to recover other unknown boundary data. The efficiency of SDRM plus MGPS was rooted in its easy numerical implementation and easy to treat the nonlinear inverse Cauchy problem.

Acknowledgement: Taiwan's National Science Council project NSC-100-2221-E-002-165-MY3 granted to the first author is highly appreciated.

References

Abbasbandy, S.; Hashemi, M. S. (2011): Group preserving scheme for the Cauchy problem of the Laplace equation. *Eng. Ana. Bound. Elem.*, vol. 35, pp. 1003-1009.

Akduman, I.; Kress, R. (2002): Electrostatic imaging via conformal mapping. *Inverse Problems*, vol. 18, pp. 1659-1672.

Andrieux, S.; Baranger, T. N.; Ben Abda, A. (2006): Solving Cauchy problems by minimizing an energy-like functional. *Inverse Problems*, vol. 22, pp. 115-133.

Aparicio, N. D.; Pidcock, M. K. (1996): The boundary inverse problem for the Laplace equation in two dimensions. *Inverse Problems*, vol. 12, pp. 565-577.

Ben Belgacem, F.; El Fekih, H. (2005): On Cauchy's problem. I. a variational Steklov-Poincaré theory. *Inverse Problems*, vol. 21, pp. 1915-1936.

Berntsson, F.; Eldén, L. (2001): Numerical solution of a Cauchy problem for the Laplace equation. *Inverse Problems*, vol. 17, pp. 839-854.

Bourgeois, L. (2005): A mixed formulation of quasi-reversibility to solve the Cauchy problem for Laplace's equation. *Inverse Problems*, vol. 21, pp. 1087-1104.

Bourgeois, L. (2006): Convergence rates for the quasi-reversibility method to solve the Cauchy problem for Laplace's equation. *Inverse Problems*, vol. 22, pp. 413-430.

Brühl, M.; Hanke, M. (2000): Numerical implementation of two noniterative methods for locating inclusions by impedance tomography. *Inverse Problems*, vol. 16, pp. 1029-1042.

Chang, J. R.; Yeih, W.; Shieh, M. H. (2001): On the modified Tikhonov's regularization method for the Cauchy problem of the Laplace equation. *J. Marine Sci. Tech.*, vol. 9, pp. 113-121.

Chapko, R.; Kress, R. (2005): A hybrid method for inverse boundary value problems in potential theory. *J. Inv. Ill-Posed Problems*, vol. 13, pp. 27-40.

Chen, K. H.; Chen, C. T.; Lee, J. F. (2009): Adaptive error estimation technique of the Trefftz method for solving the over-specified boundary value problem. *Eng. Anal. Bound. Elem.*, vol. 33, pp. 966-982.

Cheng, H.; Fu, C. L.; Feng, X. L. (2011): An optimal filtering method for the Cauchy problem of the Helmholtz equation. *Appl. Math. Lett.*, vol. 24, pp. 958-964.

Chi, C. C.; Yeih, W.; Liu, C.-S. (2009): A novel method for solving the Cauchy problem of Laplace equation using the fictitious time integration method. *CMES: Computer Modeling in Engineering & Sciences*, vol. 47, pp. 167-190.

Cimetière, A.; Delvare, F.; Jaoua, M.; Pons, F. (2001): Solution of the Cauchy problem using iterated Tikhonov regularization. *Inverse Problems*, vol. 17, pp. 553-570.

Essaouini, M.; Nachaoui, A.; Hajji, S. E. (2004): Numerical method for solving a class of nonlinear elliptic inverse problems. *J. Comp. Appl. Math.*, vol. 162, pp. 165-181.

Fang, W.; Lu, M. (2004): A fast collocation method for an inverse boundary value problem. *Int. J. Numer. Meth. Eng.*, vol. 21, pp. 1563-1585.

Fu, C. L.; Li, H. F.; Qian, Z.; Xiong, X. T. (2008): Fourier regularization method for solving a Cauchy problem for the Laplace equation. *Inv. Prob. Sci. Eng.*, vol. 16, pp. 159-169.

Inglese, G. (1997): In inverse problem in corrosion detection. *Inverse Problems*, vol. 13, pp. 1425-1438.

Johansson, T.; Marin, L. (2010): Relaxation of alternating iterative algorithms for the Cauchy problem associated with the modified Helmholtz equation. *CMC: Comput. Mater. Continu.*, vol. 13, pp. 153-168.

Jourhmane, M.; Lesnic, D.; Mera, N. S. (2004): Relaxation procedures for an iterative algorithm for solving the Cauchy problem for the Laplace equation. *Eng. Anal. Bound. Elem.*, vol. 28, pp. 655-665.

Jourhmane, M.; Nachaoui, A. (1999): An alternating method for an inverse Cauchy problem. *Num. Algor.*, vol. 21, pp. 247-260.

Jourhmane, M.; Nachaoui, A. (2002): Convergence of an alternating method to solve the Cauchy problem for Poisson's equation. *Appl. Anal.*, vol. 81, pp. 1065-1083.

Kaup, P. G.; Santosa, F.; Vogelius, M. (1996): Method for imaging corrosion damage in thin plates from electrostatic data. *Inverse Problems*, vol. 12, pp. 279-

293.

Knowles, I. (1998): A variational algorithm for electrical impedance tomography. *Inverse Problems*, vol. 14, pp. 1513-1525.

Kress, R. (2004): Inverse Dirichlet problem and conformal mapping. *Math. Comput. Simul.*, vol. 66, pp. 255-265.

Ling, L.; Takeuchi, T. (2008): Boundary control for inverse Cauchy problem of the Laplace equations. *CMES: Computer Modeling in Engineering & Sciences*, vol. 29, pp. 45-54.

Liu, C.-S. (2001): Cone of non-linear dynamical system and group preserving schemes. *Int. J. Non-Linear Mech.*, vol. 36, pp. 1047-1068.

Liu, C.-S. (2004): Group preserving scheme for backward heat conduction problems. *Int. J. Heat Mass Transfer*, vol. 47, pp. 2567-2576.

Liu, C.-S. (2008a): A modified collocation Trefftz method for the inverse Cauchy problem of Laplace equation. *Eng. Anal. Bound. Elem.*, vol. 32, pp. 778-785.

Liu, C.-S. (2008b): A highly accurate MCTM for inverse Cauchy problems of Laplace equation in arbitrary plane domains. *CMES: Computer Modeling in Engineering & Sciences*, vol. 35, pp. 91-111.

Liu, C.-S. (2008c): A highly accurate MCTM for direct and inverse problems of biharmonic equation in arbitrary plane domains. *CMES: Computer Modeling in Engineering & Sciences*, vol. 30, pp. 65-75.

Liu, C.-S. (2010a): The Fictitious Time Integration Method to Solve the Space- and Time-Fractional Burgers Equations. *CMC: Computers, Materials & Continua*, vol. 15, no. 3, pp. 221-240.

Liu, C.-S. (2010b): A Lie-Group Adaptive Method for Imaging a Space-Dependent Rigidity Coefficient in an Inverse Scattering Problem of Wave Propagation. *CMC: Computers, Materials & Continua*, vol. 18, no. 1, pp. 1-20.

Liu, C.-S. (2011): An analytical method for the inverse Cauchy problem of Laplace equation in a rectangular plate. *J. Mech.*, doi:10.1017/jmech.2011.1.

Liu, C.-S.; Atluri, S. N. (2010): An Iterative and Adaptive Lie-Group Method for Solving the Calderón Inverse Problem. *CMES: Computer Modeling in Engineering & Sciences*, vol. 64, no. 3, pp. 299-326.

Liu, C.-S.; Chang, C. W. (2012): A novel mixed group preserving scheme for the inverse Cauchy problem of elliptic equations in annular domains. *Eng. Anal. Bound. Elem.*, vol. 36, pp. 211-219.

Liu, C.-S.; Yeih, W.; Atluri, S. N. (2010): An Enhanced Fictitious Time Integration Method for Non-Linear Algebraic Equations With Multiple Solutions: Boundary Layer, Boundary Value and Eigenvalue Problems. *CMES: Computer Modeling in Engineering & Sciences*, vol. 59, no. 3, pp. 301-324.

Liu, C.-S.; Yeih, W.; Kuo, C.-L. Atluri, S. N. (2009): A Scalar Homotopy Method for Solving an Over/Under-Determined System of Non-Linear Algebraic Equations. *CMES: Computer Modeling in Engineering & Sciences*, vol. 53, no. 1, pp. 47-72.

Liu, C.-S.; Chang, C. W.; Chang, J. R. (2006): Past cone dynamics and backward group preserving schemes for backward heat conduction problems. *CMES: Computer Modeling in Engineering & Sciences*, vol. 12, pp. 67-81.

Marin, L. (2008): The method of fundamental solutions for inverse problem associated with the steady-state heat conduction in the presence of sources. *CMES: Computer Modeling in Engineering & Sciences*, vol. 30, pp. 99-122.

Marin, L. (2009): An iterative MFS algorithm for the Cauchy problem associated with the Laplace equation. *CMES: Computer Modeling in Engineering & Sciences*, vol. 48, pp. 121-152.

Mera, N. S.; Elliott, L.; Ingham, D. B.; Lesnic, D. (2000): The boundary element solution of the Cauchy steady heat conduction problem in an anisotropic medium. *Int. J. Num. Meth. Eng.*, vol. 49, pp. 481-499.

Nachaoui, A. (2004): Numerical linear algebra for reconstruction inverse problems. *J. Comp. Appl. Math.*, vol. 162, pp. 147-164.

Qian, A.; Fu, C. L.; Xiong, X. T. (2006): Fourth-order modified method for the Cauchy problem for the Laplace equation. *J. Comp. Appl. Math.*, vol. 192, pp. 205-218.

Qian, A.; Wu, Y. (2009): A computational method for a Cauchy problem of Laplace's equation. *Appl. Math. Comput.*, vol. 207, pp. 478-485.

Qin, H. H.; Wei, T. (2009): Modified regularization method for the Cauchy problem of the Helmholtz equation. *Appl. Math. Model.*, vol. 33, pp. 2334-2348.

Qin, H. H.; Wei, T.; Shi, R. (2009): Modified Tikhonov regularization method for the Cauchy problem of the Helmholtz equation. *J. Comp. Appl. Math.*, vol. 224, pp. 39-53.

Shigeta, T.; Young, D. L. (2009): Method of fundamental solutions with optimal regularization techniques for the Cauchy problem of the Laplace equation with singular points. *J. Comp. Phys.*, vol. 228, pp. 1903-1915.

Slodička, M.; Van Keer, R. (2004): A numerical approach for the determination of a missing boundary data in elliptic problems. *Appl. Math. Comp.*, vol. 147, pp. 569-580.

Tuan, N. H.; Trong, D. D.; Quan, P. H. (2010): A note on a Cauchy problem for the Laplace equation: regularization and error estimates. *Appl. Math. Comp.*, vol. 217, pp. 2913-2922.

Wei, T.; Hon, Y. C.; Ling, T. (2007): Method of fundamental solutions with regularization techniques for Cauchy problems of elliptic operators. *Eng. Anal. Bound. Elem.*, vol. 31, pp. 373-385.

Xiong, X. T.; Fu, C. L. (2006): Central difference regularization method for the Cauchy problem of the Laplace's equation. *Appl. Math. Comp.*, vol. 181, pp. 675-684.

Zhang, H. W.; Qin, H. H.; Wei, T. (2011): A quasi-reversibility regularization method for the Cauchy problem of the Helmholtz equation. *Int. J. Computer Math.*, vol. 88, pp. 839-850.